Research Article

Journal of RAMAN SPECTROSCOPY

Received: 17 March 2009 Accepted: 21 June 2009 Published online in Wiley Interscience: 6 October 2009

(www.interscience.wiley.com) DOI 10.1002/jrs.2449

Raman spectroscopic characterization of a thiophene-based active material for resistive organic nonvolatile memories

Daniele Fazzi,[a] Eleonora Valeria Canesi,[a] Chiara Bertarelli,[a] Chiara Castiglioni,[a]* Fabrizia Negri[b] and Giuseppe Zerbi[a]

A combined theoretical and experimental Raman study is presented on a diphenyl bithiophene molecule known as a good candidate for the development of organic nonvolatile memory devices. Spectroscopic markers suitable to distinguish the different stable conformers of the molecule have been predicted and detected. The combined analysis of theoretical and experimental Raman spectra recorded in solution indicates that at room temperature a dynamical equilibrium, characterized by interconversion between the two more stable conformers (namely *trans* and *cis*), takes place and that the more populated species is the *cis* form. Referring to the solid phase instead, Raman spectra of single-crystal samples show the presence of the only *trans* conformer, as confirmed by X-ray measurements. Finally, Raman spectra of thin films, as those used for the memory device, were collected; samples just deposited from solution and after few hours from the deposition were analyzed. Following the evolution of selective spectroscopic Raman markers, an isomerization process from the abundant *cis* (as-deposited) to the totally *trans* (after few hours) conformer in the solid phase was detected. These results open the way to the identification of the molecular isomers present in the thin film of the memory cell and finally of the active molecular species involved in the switching mechanism of the operating device.

Supporting information may be found in the online version of this article.

Keywords: diphenyl bithiophene; Raman markers; DFT; isomerization process; resistive organic memory

Introduction

Recent and emerging applications in organic electronics are represented by molecular switches and organic memories.[1,2] An innovative field is that of resistive nonvolatile organic memories (NVM), where, by applying a suitable voltage (threshold bias, V_{th}) to the device electrodes, a change in the electrical conductivity of the organic material is obtained, going from a low conductive state (OFF state of the memory cell) to a higher one (ON state). By cycling the bias between proper threshold values, the organic material can be written on and erased many times working as a random access memory (RAM) or can be written on once and read many times (WORM memory).[3]

This property, in which two states with different conductivity triggered by a proper electric field are present, is called *electrical bistability*, and several experimental studies have been carried out to define the key parameters (at the molecular level) governing the phenomenon and the device performances.[4–6] Variations in conductivity have been explained in terms of structural rearrangements[7] (conformational changes) or as induced by redox processes.[8–11]

Since the electronic properties of organic materials (i.e. charge mobility or energy transport) are strongly sensitive both to the single-molecular structure (*intra*-molecular properties) and to the material morphology (*inter*-molecular properties) in the solid state, the understanding of such features, in terms of (1) molecular structures, (2) stable conformers and their stabilization energies, and (3) occurrence of crystalline phases and crystal packing[12–14] is of particular relevance.

Raman spectroscopy (and in general vibrational spectroscopy) plays a key role in the study of molecular structure and structure–property relationships. It contributes to the material's characterization at the level of single molecule, but it is also sensitive to the supra molecular organization. Moreover, it provides relevant information for the understanding of how electronic processes in organic materials are governed and modulated by structural and vibrational properties.[15] Vibrational spectroscopy has been also used for the *in situ* characterization of organic electronic devices,[16,17] confirming its relevant contribution to the understanding of the molecular physics beyond the device operation involving electronic mechanisms, such as charge injection from the electrode to the organic film and charge transport across the device.[18]

In this work, we carried out a joint experimental and theoretical Raman study to investigate the more stable conformers and their Raman markers of a molecule, which belongs to the class of diphenyl bithiophenes (DPBTs). DPBTs, synthesized as the so-called

* *Correspondence to: Chiara Castiglioni, Dipartimento di Chimica, Materiali e Ingegneria Chimica 'G. Natta', Politecnico di Milano, P.zza Leonardo da Vinci 32, 20133 Milano, Italy, and INSTM, UdR Politecnico di Milano, Italy. E-mail: chiara.castiglioni@polimi.it*

a *Dipartimento di Chimica, Materiali e Ingegneria Chimica 'G. Natta', Politecnico di Milano, 20133 Milano, Italy, and INSTM, UdR Politecnico di Milano, Italy*

b *Dipartimento di Chimica 'G. Ciamician', Università di Bologna, 40126 Bologna, Italy, and INSTM, UdR Bologna, Italy*

Journal of RAMAN SPECTROSCOPY

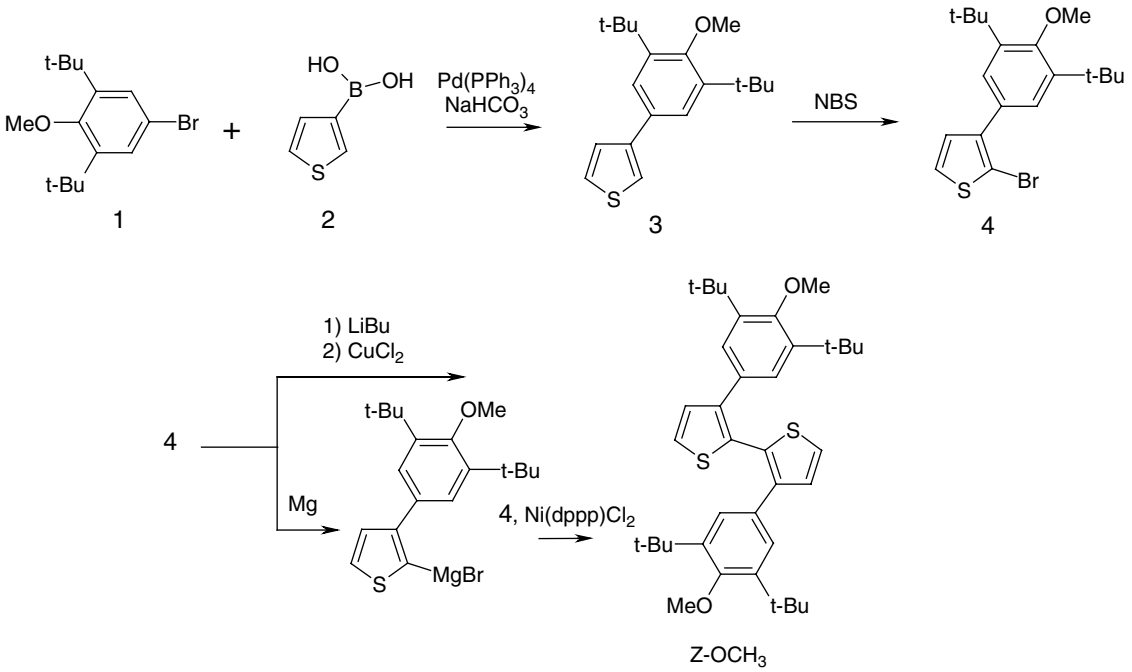

Figure 1. Synthesis of Z-OCH_3 compound.

'linear' (L) or 'Z' shape isomers,[19] are good candidates for resistive memory applications.[5,6] A recent theoretical investigation[20] suggested a possible mechanism for their electrical bistability behavior. In Ref. [20] we carried out a complete conformational study, finding the more stable conformers of DPBT molecules (namely *trans* and *cis* for both L and Z isomers). For the Z isomer, the theoretical results matched favorably the structural parameters obtained by X-ray measurements carried out on single-crystal samples. From density functional theory (DFT) simulations, the energy difference between *trans* and *cis* conformers turned out to be negligible, and the energy barrier for *cis*–*trans* interconversion was predicted to be very small (a few kcal/mol).

The vibrational study here reported refers to the Z structural isomer with the OCH_3 functional group on the phenyl moieties (hereafter labeled as Z-OCH_3, see Fig. 1), and has the purpose of finding spectroscopic markers that can be used as fingerprint to detect the existence in the sample of different stable conformers.

The paper is organized as follows: first we outline the synthetic procedure employed to prepare Z-OCH_3 molecule. Then, we briefly summarize the results of the conformational analysis reported in Ref. [20] and we analyze the simulated Raman spectra (*in vacuo*) of the more stable conformers of Z-OCH_3 in order (1) to define their spectroscopic differences and (2) to find *suitable* spectral regions for the identification of those spectroscopic markers useful for the identification of *trans, cis,* or any other Z-OCH_3 stable conformer.

Once the markers have been identified, a direct comparison between the theoretical results and the experimental Raman spectra of DPBT collected in different solvents allows us (1) to study the effect of different environments on the Raman features of Z-OCH_3 DPBT and (2) to estimate, by using a simple fit model, the relative populations of the two major conformers.

We then analyze the Raman spectra of a Z-OCH_3 single crystal which has been fully characterized in terms of molecular structure as shown by a previous X-ray analysis.[20]

Finally, we describe some preliminary outcomes of the Raman study on Z–OCH_3 thin films, which are strictly related to the active layer in the memory devices.

Methods

Computational details

Z-OCH_3 structures, vibrational wavenumbers, and intensities are obtained by using the three-parameter exchange correlation functional B3LYP[21] with the split-valence Pople basis set 6-31G**,[22] by using the Gaussian03 code.[23] The choice of B3LYP/6-31G** level of theory is related to the fact that (1) a good match between experimental X-ray and theoretical structural parameters (in terms of bond lengths and angles) has been already obtained[20] and (2) by using a proper scaling factor applied to the vibrational wavenumbers[24] good agreement between experimental and theoretical vibrational spectra is reached.

A fitting procedure that maximizes the overlap between theoretical and experimental Raman spectra has been devised to obtain an estimate of the relative populations of the two more stable *trans* and *cis* Z-OCH_3 conformers. The fitting procedure is based on a weighted sum of the calculated Raman spectra of the *cis* and the *trans* conformers, where bands originating by a single vibrational transition are described by a Lorentzian function characterized by its peak wavenumber and area, which are given by theoretical wavenumber ν_i and intensity I_i, respectively.

Once a suitable wavelength range is selected, the theoretical spectrum (S) is built as reported in Eqn (1):

$$S_{\mathrm{trans/cis}}(\nu) = \sum_i I_i L_i(\nu) \qquad (1)$$

in Eqn (1) I_i is the Raman intensity of the ith normal mode obtained from quantum chemical simulations and L_i is a Lorentzian function

defined as

$$L_i(\nu) = (\Gamma/2\pi)/[(\nu - \nu_i{\cdot}t)^2 + (\Gamma/2)^2] \quad (2)$$

where Γ is the full width at half-maximum (FWHM), ν_i is the vibrational wavenumber of the *i*th normal mode and *t* is the wavenumber scaling factor. In order to mimic the Raman spectra in solution, where probably both *trans* and *cis* conformers are present, the analogous theoretical Raman spectra is obtained by a linear combination of the two $S_{trans}(\nu)$ and $S_{cis}(\nu)$ spectra:

$$S(\nu) = c_{trans}{\cdot}S_{trans}(\nu) + c_{cis}{\cdot}S_{cis}(\nu) \quad (3)$$

where c_{trans} and c_{cis} are the relative conformer populations. The theoretical Raman spectra $S(\nu)$ is then fitted with the experimental one by following a minimization mean-square errors procedure. The fitted parameters are the relative population c_{trans} and c_{cis}, the wavenumber scaling factor *t*, and the Lorentzian's width Γ.

Experimental

Procedures for the synthesis of the Z-OCH_3 and the intermediates are reported in the Supporting Information. Unless otherwise specified, all reagents, catalysts, and reagent-grade solvents were commercial (Sigma Aldrich, Panreac), while anhydrous diethyl ether was dried over a Na–K alloy. All the molecules have been characterized with ^{1}H-NMR spectroscopy.

All solvents used for the spectroscopic analysis were purchased by Sigma Aldrich or J.T. Baker and used without further treatments. A solution concentration around 10^{-1} M was chosen, thus providing a good signal-to-noise spectral ratio and avoiding aggregation phenomena.
Crystals of Z-OCH_3 were obtained by slow evaporation from solution.

Thin films were obtained on glass substrates using both casting and spin-coating (1500 rpm) techniques, from chloroform solutions with a concentration of 60 mg/ml.

FT-Raman spectra of samples in solution or in crystal powder were recorded with a Nicolet FT-Raman Nexus NXR 9650 instrument, which employs a Nd/YAG laser with excitation at $\lambda = 1064$ nm. For each spectrum, 512 scans were acquired with 2 cm^{-1} resolution and 800 mW of laser power. No spectral changes induced by the laser were observed during the spectra acquisitions. The Raman wavenumber range considered is between 100 and 3700 cm^{-1}. Intensity was corrected with white-light internal correction. Both liquid and solid samples were sealed in NMR tubes suitable for the Raman spectrometer. For thin-film samples, Raman spectra were recorded with a Horiba Jobin Yvon Labram HR800 instrument using the 514.5 nm line of an argon ion laser for excitation and equipped with a microscope that can be focussed on specific areas of the sample with a resolution of the order of micrometers, thus allowing distinguishing the different regions of the film. The laser power was some tens of milliwatts. In order to evaluate the possible effect of the laser excitation on the spectral features of the material, the same setup was used also for some of the crystalline samples analyzed with FT-Raman. No significant differences in terms of wavenumber shifts were detected.

Results and Discussion

Synthesis

The molecule involved in this study is 3,3′-bis(3,5-di-*tert*-butyl-4-methoxyphenyl)-2,2′-bithiophene (Z-OCH_3, Fig. 1, in which the synthetic route is reported). The synthesis consists in the Suzuki coupling of 1-methoxy-2,6-di-*tert*-butyl-4-bromo benzene (**1**) with 3-thiophen boronic acid (**2**) to give half a molecule. The resulting intermediate (**3**) is brominated in 2-position with *N*-bromosuccinimide: the reaction was conducted in different solvents, such as carbon tetrachloride or a mixture of acetic acid : chloroform = 1 : 1, with comparable yield but a difference in the reaction time resulted, the latter being much faster than the former.[25]

Two different coupling strategies were followed to yield the targeted molecule: intermediate (**4**) was lithiated with buthyllithium and subsequently coupled with $CuCl_2$[19], or the correspondent Grignard reagent was reached from (**4**) followed by a Kumada coupling, catalyzed by Ni(dppp)Cl_2. Following this second route, an enhancement of the yield was obtained, going from 33% to 67%. These syntheses were preferred to the Suzuki–Miyaura coupling recently reported[26] because of the difficulty to obtain 3,5-di-*tert*-butyl-4-hydroxyphenylboronic acid as a pure product in high yields.

See the Supporting Information for experimental procedures and ^{1}H-NMR spectra.

Theoretical results

Because of the bulky *tert* butyl (tBu) substituents and of the presence of relatively flexible exocyclic CC bonds, Z-OCH_3 is characterized by a complex and conformationally flexible nonplanar structure. As reported in Ref. [20], from a detailed conformational analysis carried out on Z-OCH_3 it turns out that, among the many possible stable conformers, only two can be selected on the basis of their energy, namely the *trans* and the *cis* forms (Fig. 2), both showing a perfect C_2 point group symmetry. From DFT calculations (*in vacuo*), the *trans* Z-OCH_3 species is more stable than the *cis* by 0.37 kcal/mol. Also, DFT simulations carried out mimicking the solution phase (by using the polarizable continuum model (PCM)[27] as implemented in the Gaussian03 code), give the *trans* form as the more stable ($\Delta E = 0.4–0.5$ kcal/mol). However, we should note that an error of the order of 1 kcal/mol in the computed relative energies of the two conformers is within the accuracy of the level of the theory (B3LYP/6-31G**) adopted in these calculations. By varying the dihedral angle (α) between the two thiophene rings, it is possible to transform the *trans* conformer to the *cis*; accordingly, we calculated the potential energy surface (PES) scan by varying α and optimizing the other internal molecular degrees of freedom at each step. The calculated energy barrier between the two conformers turned out to be ≈5 kcal/mol. From these results we concluded that, at room temperature and in solution, the *trans*–*cis* isomerization process should easily occur for Z-OCH_3. However, this conclusion has not been supported yet by any systematic experimental study. To further clarify this point, we simulated the Raman spectra of both *trans* and *cis* Z-OCH_3 conformers in order to study their vibrational properties and to identify suitable spectral regions in which the two forms might show selective spectroscopic markers. This will be particularly useful for their characterization and recognition both in solution and in the solid phase.

In order to point out the relevant spectroscopic markers in the simulated Raman spectra, we consider here two regions, namely spectral region I: 1700–1350 cm^{-1} and spectral region II: 650–400 cm^{-1}. In Fig. 3 we report the unscaled theoretical *trans* and *cis* Z–OCH_3 Raman spectra in this two regions.

From the spectral region I (Fig. 3a) the following observations can be made: (1) the *trans* form shows higher Raman intensity

Journal of RAMAN SPECTROSCOPY

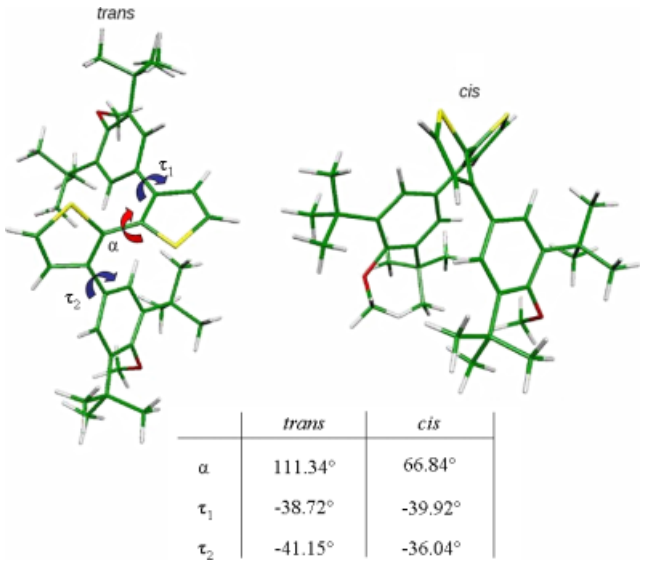

	trans	cis
α	111.34°	66.84°
τ_1	-38.72°	-39.92°
τ_2	-41.15°	-36.04°

Figure 2. Molecular sketch of the *trans* and *cis* conformer of Z-OCH_3 with the indication of the main dihedral angles involved in the conformational study. Optimized molecular structures as obtained by B3LYP/6-31G** simulations. For a detailed analysis of the geometry see Ref. [20].

than the *cis*; (2) the intensity ratios of the three Raman bands, from 1612 to 1566 cm^{-1} (bands B, C, D, Fig. 3a), are different in the two conformers; and (3) a slight blue shift of 5 cm^{-1} is observed for the *cis* band at 1575 cm^{-1} (D) with respect to the corresponding band of the *trans* form.

The detailed normal mode analysis (reported in the Supporting Information) reveals that, for both the *trans* and *cis* species, the Raman active vibrations in this spectral range correspond to C=C and C–C bond stretching, which are either localized onto the two phenyl groups or delocalized along the whole molecular backbone, following the π-electrons delocalization path.

Accordingly, band A ($\nu_A = 1640\ cm^{-1}$) corresponds to two accidentally degenerate transitions for both *trans* and *cis* conformers, consisting of a symmetric (*A* species referring to the C_2 point group) and an antisymmetric (*B* species) vibration localized onto the phenyl moieties; as sketched in the Supporting Information (Fig. S1), this vibration can be described as an oscillation of the phenyl rings between an aromatic and a more quinoid structure. Its intensity is not surprising since the normal mode localized on the phenyl rings bears a parentage with the Raman active ν_8 (Wilson notation) normal mode of benzene or even with the G band of fused polycyclic aromatic hydrocarbons and ultimately of graphite.[28,29]

The normal mode of *A* species has a higher Raman intensity than that of the *B* species by a factor of 1.5. Bands B ($\nu_B = 1612\ cm^{-1}$, *A* species), C ($\nu_C = 1593\ cm^{-1}$, *A* species), and D ($\nu_D = 1566\ cm^{-1}$, *B* species), whose eigenvectors are reported in Supporting Information (Fig. S2), are related to alternating CC stretching and shrinking along the π-conjugation path involving the whole molecular backbone, while band E ($\nu_E = 1500\ cm^{-1}$, *A* species) is the in-phase CC stretching and shrinking more localized on the bithiophene unit (see Fig. S3 in the Supporting Information). These bands (B–E) can be referred to the well known $\mathcal{R}$-modes, consisting of alternated stretching and shrinking of adjacent CC bonds belonging to a sequence of carbon atoms bearing conjugated π electrons.[30] In the molecule under study, there are different possible conjugation paths for π electrons, namely a CC bond sequence along the whole molecular backbone (thus involving CC bonds of the bithiophene and phenyl units) and a CC bond sequence confined to the bithiophene unit. Accordingly, normal vibrations are either delocalized along the π-conjugation path on the molecular backbone (modes B–C–D, bonds sequence 1–11 see Fig.4) or confined to the bithiophene unit (mode E, bonds sequence 12–13–7–6–5–14–15, see Fig. 4). The strong Raman activity of these vibrational transitions and, in particular, the relevance of vibrations involving CC stretchings belonging to a chain of conjugated thiophene rings (as for band E) have been already observed and described for thiophene-based molecular systems[31,32] and generally for other π-conjugated molecules[33,34] in the framework of the effective conjugation coordinate (ECC) theory.[35,36]

In Fig. 4, the computed values of the derivative of the polarizability tensor's trace with respect to the CC bond stretching ($\partial<\alpha>/\partial R_{CC}$; $<\alpha>$ = Tr [α]) are reported for the two different π conjugation paths, as mentioned above. The sign of $\partial<\alpha>/\partial R_{CC}$ oscillates from positive to negative values, with the only exception of the next-to-last bond along the sequence. This behavior is responsible of the large $\partial\alpha/\partial Q$ value (and hence of the Raman intensity) shown by normal modes, which can be described as a collective out-of-phase CC stretching, namely the $\mathcal{R}$-vibrations (Fig. 4). Moreover, it is interesting to note that all the $\partial<\alpha>/\partial R_{CC}$ values are slightly larger in the *trans* conformer than in the *cis*, a fact which justifies the larger intensity of the *trans* Raman pattern with respect to the *cis*, in the spectral region I.

For region II (650–400 cm^{-1}, Fig. 3b), the theoretical Raman spectra of *trans* and *cis* conformers show relevant differences in their pattern. Bands *a* ($\nu_a = 500\ cm^{-1}$) and *b* ($\nu_b = 600\ cm^{-1}$) are stronger for the *trans* conformer than for the *cis*. (The Raman intensities of the II spectral region are 2 orders of magnitude lower than those of the I region (1700–1450 cm^{-1})). Band *a* at 500 cm^{-1} (*A* species, Fig. S4) is highly sensitive to the different molecular structures of the Z-OCH_3; the analysis of the computed normal mode eigenvectors shows that the associated vibrational displacements involve a torsional motion around the C–C bond linking the two thiophene rings. Interestingly, this 500 cm^{-1} mode has larger Raman intensity for the *trans* than the *cis* form: its relative intensity can be proposed as a Raman marker to probe the occurrence of *trans, cis,* or both conformers. As a further proof of the correctness of our assignment, we have simulated also the Raman spectra of a molecular moiety corresponding to one half Z-OCH_3, namely the intermediate **3** in Fig. 1, thus excluding the degree of freedom related to the variation of the dihedral angle between thiophene rings. Indeed, in the predicted Raman spectrum of this compound, the *a* band localized at 500 cm^{-1} disappears.

Band *b* at 600 cm^{-1} consists of two degenerate modes, one corresponding to the *A* species (high Raman intensity) and one to the *B* species (low Raman intensity) related to out-of-plane modes localized on the phenyl-thiophene moiety, as reported in Fig. S5.

In the 550 cm^{-1} region, broad features for both *trans* and *cis* are observed showing different intensity patterns; the normal mode analysis shows that the vibrations involved are related to out-of-plane vibrations localized on the phenyl and/or on the *tert*-butyl moieties differently coupled in the normal modes of the two conformers.

From these theoretical results we can conclude that: (1) There are many differences, in terms of bands intensity and wavenumber shifts, in the Raman spectra of *trans* and *cis* Z-OCH_3 conformers; (2) While in the region I there is a broad change of the spectral pattern and it is difficult to find simple and well-defined makers for

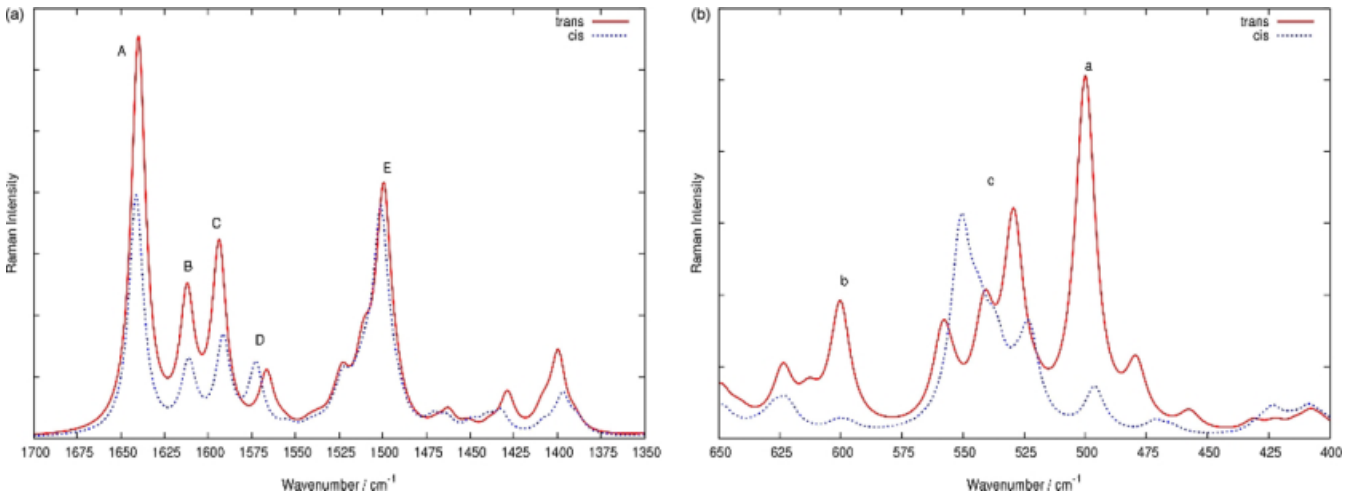

Figure 3. Simulated Raman spectra: (a) I spectral region, 1700–1350 cm^{-1} and (b) II spectral region, 650–400 cm^{-1} of both Z-OCH_3 *trans* (solid line) and *cis* (dotted line) conformers (unscaled B3LYP/6-31G** wavenumber).

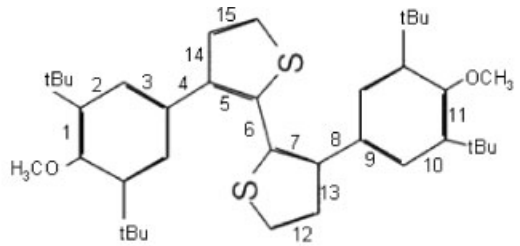

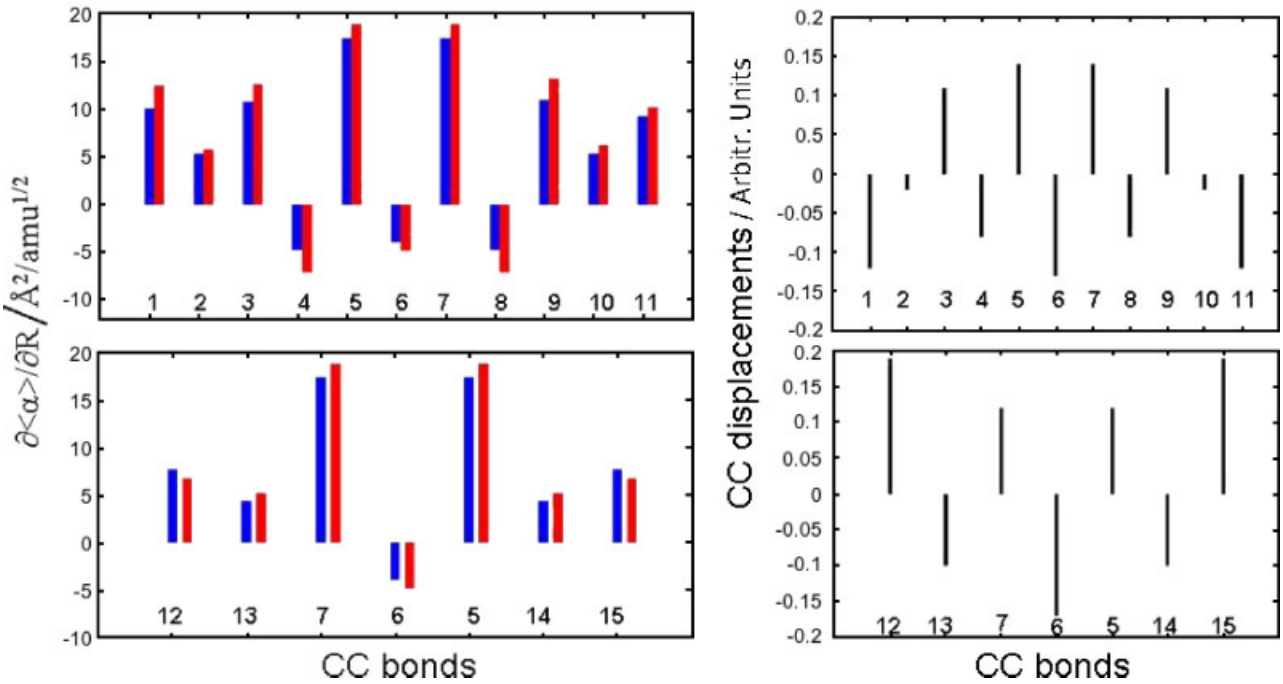

Figure 4. Z-OCH_3 molecular structure with the two conjugation paths: 1–11 and 12–13–7–6–5–14–15. Upper panel: theoretical values of the derivative of the polarizability tensor's trace with respect to the CC bond stretching (left) and the corresponding –mode (band C, $\nu_C = 1593$ cm^{-1}) along the first conjugation path (right). Bottom panel: the same results displayed along the bithiophene moiety (12-13-7-6-5-14-15), and the –mode localized onto the thiophene rings (band E, $\nu_E = 1500$ cm^{-1}). Red bars for *trans* conformer and blue bar for *cis*.

Journal of RAMAN SPECTROSCOPY

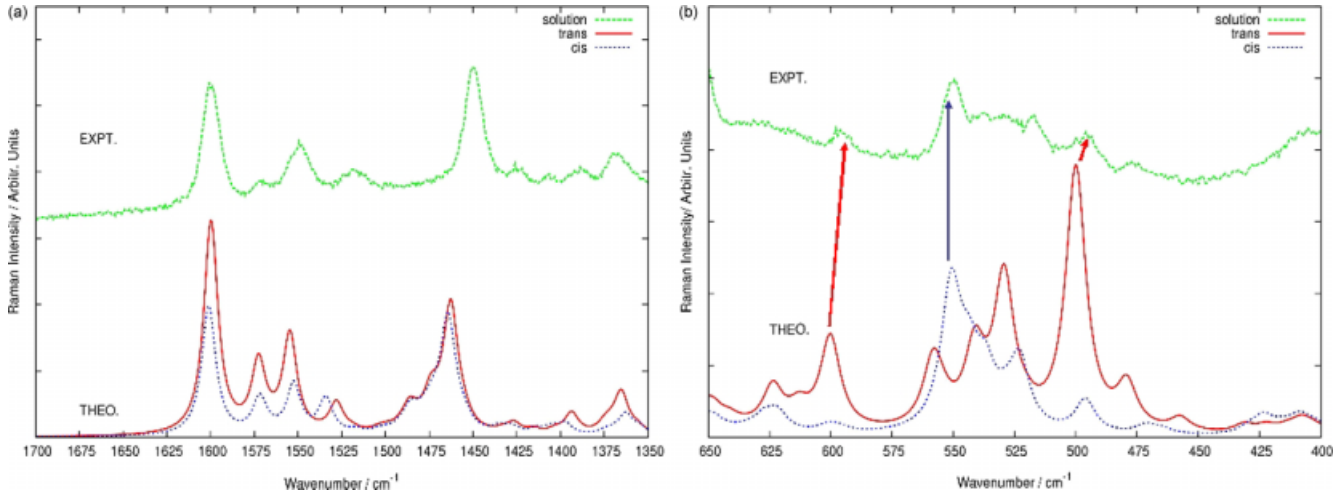

Figure 5. Comparison between experimental (top) Raman spectra (chloroform solution, dotted line) and simulated (bottom) spectra of Z-OCH_3, *trans* (solid line) and *cis* (dotted line) conformers. (a) I spectral region, 1700–1350 cm^{-1} and (b) II spectral region, 650–400 cm^{-1}. Theoretical frequencies are scaled in the I region by a factor of 0.9755 and are unscaled in the II region.

a conformational diagnosis, the spectral region II (650–400 cm^{-1}) is the most suitable region for the detection (through the analysis of the experimental spectra) of the different conformers in real samples and possibly for a semiquantitative determination of their relative populations by means of fitting procedures (see below). Spectroscopic markers in this region turn out to be the bands *a* (ν_a = 500 cm^{-1}), *b* (ν_b = 600 cm^{-1}), and the intensity pattern around 550 cm^{-1}.

Based on the conclusions of our theoretical analysis, the experimental data will be analyzed in the wavenumber range identified through the modeling, namely regions I and II.

Experimental Raman spectra in solution

The two reference regions of the FT-Raman spectrum of a solution of Z-OCH_3 in chloroform are reported in Fig. 5 and compared with the simulations in which all frequencies of the region I are scaled by a suitable factor (0.9755). In the spectra of solutions, the signals of the solvent have been subtracted.

The comparison between the experimental Raman spectra and the theoretical results does not show evidence of any dominant species between the two conformers, thus indicating that both forms can occur in solution at room temperature. Both the band pattern around 1500 cm^{-1} and the broad experimental intensity pattern around 550 cm^{-1} well match with those of the simulated *cis* form, but the observation of weaker Raman bands around 600 and 500 cm^{-1} (red arrows in Fig. 5b) suggests the existence of also the *trans* species.

The different relative intensities of the features in the region between 480 and 600 cm^{-1} make possible a study on the relative conformers population: the fitting procedure gives a *cis : trans* ratio of *ca* 4 : 1 (Fig. S6 of the Supporting Information).

This ratio suggests that the *cis* form is more stable than the *trans* one, at least in solution. Considering a classical Boltzmann distribution, a *cis : trans* ratio of *ca* 4 : 1 at room temperature implies an energy difference of 0.8 kcal/mol in favour of the *cis* species, consistent with the theoretical results previously discussed.

In order to explore whether the relative conformers population and stabilization energies estimated are influenced by the environment, Raman spectra of Z-OCH_3 in different solvents were analyzed. The solvents considered were acetone, dichloromethane, tetrahydrofuran (THF), diethyl ether, and *n*-hexane, which cover a quite wide range of values of dielectric constants and dipole moments (as reported in Table 1 of the Supporting Information).

Despite the different properties of the solvents, the differences observed in the conformer population ratio after the fitting procedure of Raman spectra are quite small and confirm the 4 : 1 *cis* to *trans* ratio for each case, thus excluding a strong correlation between the stability of the two molecular structures and the chemical-physical properties of the environment. We can conclude that the dielectric constant and the permanent dipole moment of the solvents have negligible effect on the stability of the conformers for the molecule Z-OCH_3 and that the *cis* form is always the dominant species in solution (Fig. S7). On the other hand, in accordance with the theoretical simulations, the values of permanent dipole moment (μ_{trans} = 0.7768 D, μ_{cis} = 0.6659 D) are not very different; this fact allows us to dismiss the hypothesis of the existence of remarkably different dipole–dipole interactions between the two conformers and the polar solvents used. Moreover, the Raman spectra simulated with the presence of solvents such as chloroform by using the PCM approach show no relevant wavenumber shifts both in the I and II region considered here.

A further support to these results has been obtained by considering the possible effect on the Raman features of Z-OCH_3 of a bad solvent: by adding portionwise methanol to a chloroform solution of Z-OCH_3, no significant differences in the Raman markers were observed until the two solvents were around 1 : 1 vol; at the saturation limit, a Z-OCH_3 precipitate as a white powder was obtained. The spectrum of this powder (see Supporting Information, Fig. S8) shows the typical markers of the *trans* isomer, in accordance with the experimental results reported in the next section.

Experimental Raman spectra in the solid state: single crystals and thin films

Single crystals were obtained through slow evaporation from concentrated solutions of Z-OCH_3 in diethyl ether. X-ray analysis[20] indicates that the crystalline structure of the molecule is the *trans* form. The result is confirmed by Raman spectroscopy; the *trans*

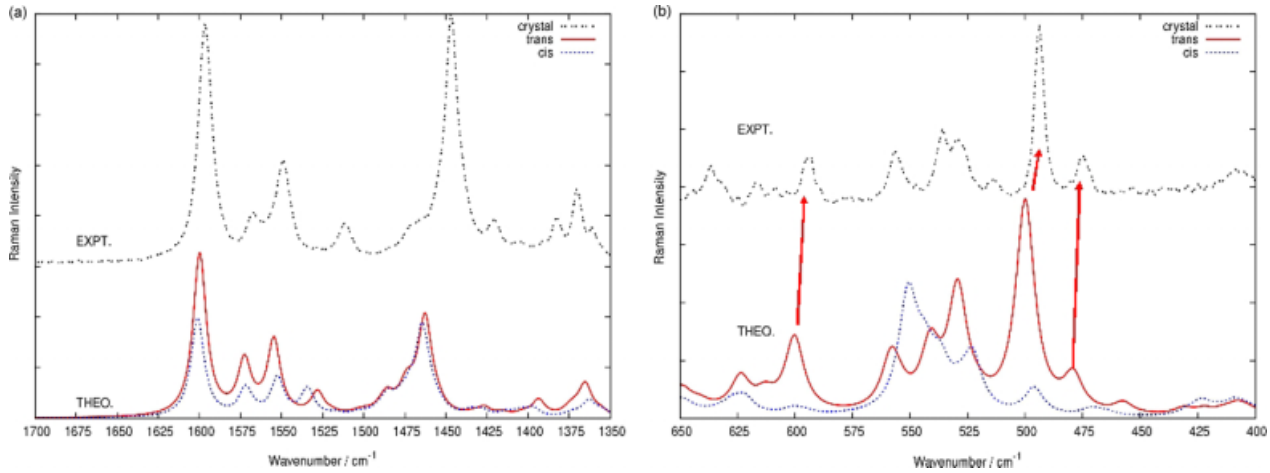

Figure 6. Comparison between experimental (single crystal obtained from diethyl ether solution, upper broken line) and simulated (bottom) spectra of Z-OCH_3, *trans* (solid line) and *cis* (dotted line) conformers. (a) I spectral region, 1700–1350 cm^{-1} and (b) II spectral region, 650–400 cm^{-1}. Theoretical frequencies are scaled in the I region by a factor of 0.9755 and are unscaled in the II region. Arrows indicate the band assignment and intensity trend for *cis* and *trans* conformer.

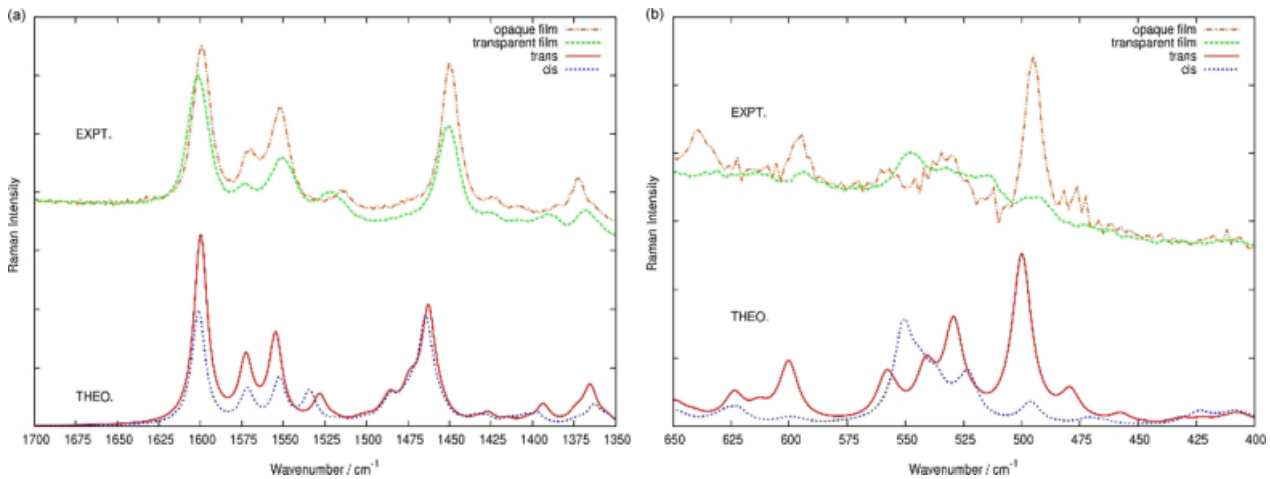

Figure 7. Comparison between experimental Raman spectra of deposited (casting) Z-OCH_3 thin film from chloroform solution (upper dotted line 'transparent') and after 24 h of exposure in air (upper broken line, 'opaque'). (a) I spectral region, 1700–1350 cm^{-1} and (b) II spectral region, 650–400 cm^{-1}. Theoretical simulated (bottom) Raman spectra of Z-OCH_3, *trans* (solid line) and *cis* (dotted line) conformers, are also reported for direct comparison.

isomer is indeed immediately recognized by considering, in the spectral region II, the sharp peak near 500 cm^{-1}, the well-defined weak band at 600 cm^{-1}, and the pattern of three bands near 550 cm^{-1} (Fig. 6b). Accordingly, for the spectral region I, we notice the red shift of the D band near 1525–1515 cm^{-1}, which is assigned to the *trans* conformer. Moreover, the intensity of the 1375 cm^{-1} band (Fig. 6a) leads to the hypothesis that the *cis* form, if present, is not the dominant one. Crystals obtained from THF and ethyl acetate provide the same Raman features, thus indicating that negligible effects result from changing the starting solution.

The same spectroscopic study was applied to thin film samples, representative of the organic layer in nonvolatile memories based on Z-OCH_3[5] in order to highlight which active species are present in the device and thus involved during the electrical process; this is certainly a key point to determine the molecular origin of the switching mechanism.

Thin films were cast from a chloroform solution to yield thicker films with respect to spin-coated layers (some microns *vs* hundreds of nanometres); this difference of around one order of magnitude allows a better signal-to-noise ratio in the Raman spectra. For both the cast and spin-coated films, a progressive transition to an opaque film, which started from nucleation sites usually located near the film boundary, was observed during time. At room conditions, this phenomenon starts a few hours after the deposition and takes some days to complete, depending on the uniformity and the extension of the film.

For these samples, the Raman spectra of transparent and opaque regions of the film were obtained with a Raman spectrometer equipped with a microscope that allowed focusing the laser line (in the visible) on specific points of the sample with a resolution of the order of micrometers. Interestingly, the transparent areas of the film provide the same features of the solution spectra reported previously (abundance of *cis* conformer, see Fig. 7b). In contrast, the opaque regions show the appearance of the bands *a* around 500 cm^{-1} and *b* at 600 cm^{-1}, typical of the *trans* conformer (Fig. 7b). These findings lead to the hypothesis that a *cis* to *trans* isomerization occurs in the solid state, starting from a

more abundant *cis* form in the film as deposited and reaching a new population dominated by the *trans* species after few hours.

At this stage of the work, the Raman analysis gives this indication: in the solid state (film), the system tends to form a crystalline phase as indicated by the observation of the specific markers of the *trans* conformer in opaque regions. On the other hand, the remarkably different Raman features of the film observed immediately after deposition, together with its transparent appearance, suggest that in the starting film the material morphology corresponds to a mainly amorphous molecular arrangement.

Conclusions

We have shown that Raman spectroscopy is a powerful key technique to characterize the conformational isomers of DPBT molecules, which have been proposed for the fabrication of nonvolatile resistive memory devices.

One structural isomer, namely Z-OCH_3, displaying two different conformers of similar stability, has been considered. From a direct comparison between experimental and simulated Raman spectra, it is apparent that unambiguous spectroscopic markers related to the presence of the *trans* or of the *cis* Z–OCH_3 conformer can be identified and rationalized in two specific spectral regions. Raman spectra of Z-OCH_3 in solution show that *trans* and *cis* conformers are both present in dynamic equilibrium. A fitting procedure based on predicted spectra indicates that in solution the relative population of the *cis* form is larger than that of *trans* form (*cis : trans* ca 4:1).

Both the X-ray analysis and the Raman spectra on single crystals, validated on the basis of the theoretical simulations, confirm the presence of the only *trans* species due to the appearance of sharp bands near 500 and 600 cm^{-1}. For the material in thin film, which is representative of the active layer of the memory devices, a solid-state rearrangement occurs. Indeed, the film as deposited shows Raman signals typical of the *cis* species (as for the solution phase), but after few hours at room temperature, the Raman spectrum clearly indicates the presence only of the *trans* conformer in some specific opaque regions of the film, testifying an isomerization of the *cis* species accompanied by a crystallization process.

Acknowledgement

This work has been partly supported by grants from the Italian Ministry of Education, University and Research through FIRB projects 'Molecular compounds and hybrid nanostructured materials with resonant and nonresonant optical properties for photonic devices' (RBNE033KMA) and from MIUR grant ex 60%.

Supporting information

Supporting information may be found in the online version of this article.

References

[1] J. Scott Campbell, L. Bozano, *Adv. Mater.* **2007**, *19*, 1452.
[2] L. Qi-Dan, L. Der-Jang, C. Zhu, D. Siu-Hung Chan, E. T. Kang, N. Koon-Gee, *Prog. Polym. Sci.* **2008**, *33*, 917.
[3] L. Qi-Dan, L. Der-Jang, Teo. E. Yeow-Hwee, C. Zhu, Siu.-Hung. Chan, E. T. Kang, N. Koon-Gee, *Polymer* **2007**, *48*, 5182.
[4] A. Bandhopadhyay, A. J. Pal, *J. Phys. Chem. B* **2003**, *107*, 2531.
[5] M. Caironi, D. Natali, M. Sampietro, C. Bertarelli, A. Bianco, A. Dundulachi, E. Canesi, G. Zerbi, *Appl. Phys. Lett.* **2006**, *89*, 243519.
[6] M. Caironi, D. Natali, E. Canesi, A. Bianco, C. Bertarelli, G. Zerbi, M. Sampietro, *Thin Solid Films* **2008**, *516*, 7680.
[7] J. Chen, M. A. Reed, A. M. Rawlett, J. M. Tour, *Science* **1999**, *286*, 1550.
[8] A. O. Solak, S. Ranganathan, T. Itoh, R. L. McCreery, *Electrochem. Solid State Lett.* **2002**, *5*, E43.
[9] A. K. Rath, A. J. Pal, *Org. Elec.* **2008**, *9*, 495.
[10] B. Mukherjee, A. J. Pal, *Org. Elec.* **2006**, *7*, 249.
[11] S. Di Motta, E. Di Donato, F. Negri, G. Orlandi, D. Fazzi, C. Castiglioni, *J. Am. Chem. Soc.* **2009**, *131*, 6591.
[12] V. Coropceanu, J. Cornil, D. A. da Silva Filho, Y. Olivier, R. Silbey, J. L. Brédas, *Chem. Rev.* **2007**, *107*, 926.
[13] A. Brillante, I. Bilotti, R. G. Della Valle, R. Venuti, M. Masino, A. Girlando, *Adv. Mater.* **2005**, *17*, 2549.
[14] E. Venuti, I. Bilotti, R. G. Della Valle, A. Brillante, P. Ranzieri, M. Masino, A. Girlando, *J. Phys. Chem. C* **2008**, *112*, 17416.
[15] H. L. Cheng, W. Y. Chou, C. W. Kuo, Y. W. Wang, Y. S. Mai, F. C. Tang, S. W. Chu, *Adv. Funct. Mater.* **2008**, *18*, 285.
[16] R. L. McCreery, J. Wu, R. P. Kalakodimiw, *Phys. Chem. Chem. Phys.* **2006**, *8*, 2572.
[17] L. G. Kaake, Y. Zou, M. J. Panzer, C. D. Frisbie, X. Y. Zhu, *J. Am. Chem. Soc.* **2007**, *129*, 7824.
[18] Q. Bao, Y. Gan, J. Li, C. M. Li, *J. Phys. Chem. C* **2008**, *112*, 19718.
[19] E. Canesi, G. Dassa, C. Botta, A. Bianco, C. Bertarelli, G. Zerbi, *Open Chem. Phys. J.* **2008**, *1*, 23.
[20] D. Fazzi, C. Castiglioni, F. Negri, C. Bertarelli, A. Famulari, S. V. Meille, G. Zerbi, *J. Phys. Chem. C* **2008**, *112*, 18628.
[21] A. D. Becke, *J. Chem. Phys.* **1993**, *98*, 5648.
[22] G. A. Petersson, A. Bennett, T. G. Tensfeldt, M. A. Al-Laham, W. A. Shirley, J. Mantzaris, *J. Chem. Phys.* **1988**, *89*, 2193.
[23] Gaussian 03, Revision C.01, M. J. Frisch, G. W. Trucks, H. B. Schlegel, G. E. Scuseria, M. A. Robb, J. R. Cheeseman, J. A. Montgomery Jr., T. Vreven, K. N. Kudin, J. C. Burant, J. M. Millam, S. S. Iyengar, J. Tomasi, V. Barone, B. Mennucci, M. Cossi, G. Scalmani, N. Rega, G. A. Petersson, H. Nakatsuji, M. Hada, M. Ehara, K. Toyota, R. Fukuda, J. Hasegawa, M. Ishida, T. Nakajima, Y. Honda, O. Kitao, H. Nakai, M. Klene, X. Li, J. E. Knox, H. P. Hratchian, J. B. Cross, V. Bakken, C. Adamo, J. Jaramillo, R. Gomperts, R. E. Stratmann, O. Yazyev, A. J. Austin, R. Cammi, C. Pomelli, J. W. Ochterski, P. Y. Ayala, K. Morokuma, G. A. Voth, P. Salvador, J. J. Dannenberg, V. G. Zakrzewski, S. Dapprich, A. D. Daniels, M. C. Strain, O. Farkas, D. K. Malick, A. D. Rabuck, K. Raghavachari, J. B. Foresman, J. V. Ortiz, Q. Cui, A. G. Baboul, S. Clifford, J. Cioslowski, B. B. Stefanov, G. Liu, A. Liashenko, P. Piskorz, I. Komaromi, R. L. Martin, D. J. Fox, T. Keith, M. A. Al-Laham, C. Y. Peng, A. Nanayakkara, M. Challacombe, P. M. W. Gill, B. Johnson, W. Chen, M. W. Wong, C. Gonzalez, J. A. Pople, Gaussian, Inc.: Wallingford, **2004**, http://www.gaussian.com/g_misc/g03/citation_g03.htm.
[24] J. P. Merrick, D. Moran, L. Radom, *J. Phys. Chem. A* **2007**, *111*, 11683.
[25] R. M. Kellogg, A. P. Schaap, E. T. Harper, H. Wynberg, *J. Org. Chem.* **1968**, *33*, 2902.
[26] H. Kurata, S. Kim, T. Fujimoto, K. Matsumoto, T. Kawase, T. Kubo, *Org. Lett.* **2008**, *10*, 3837.
[27] J. Tomasi, B. Mennucci, R. Cammi, *Chem. Rev.* **2005**, *105*, 2999.
[28] F. Negri, C. Castiglioni, M. Tommasini, G. Zerbi, *J. Phys. Chem. A* **2002**, *106*, 3306.
[29] N. C. Handy, P. E. Maslen, R. D. Amos, J. S. Andrews, C. W. Murray, G. J. Laming, *Chem. Phys. Lett.* **1992**, *192*, 506.
[30] G. Zerbi, *Vibrational Spectroscopy of Polymers: Principles and Practice* (Eds.: N. Everall, J. M. Chalmers, P. R. Griffiths) John Wiley and Sons: Chichester, **2007**.
[31] E. Agosti, M. Rivola, V. Hernandez, M. Del Zoppo, G. Zerbi, *Synth. Met.* **1999**, *100*, 101.
[32] A. Milani, L. Brambilla, M. Del Zoppo, G. Zerbi, *J. Phys. Chem. B* **2007**, *111*, 1271.
[33] F. Negri, E. di Donato, M. Tommasini, C. Castiglioni, G. Zerbi, K. Muellen, *J. Chem. Phys.* **2004**, *120*, 11889.
[34] C. Castiglioni, M. Tommasini, G. Zerbi, *Phil. Trans. R. Soc. Lond. A* **2004**, *362*, 2425.
[35] C. Castiglioni, M. Gussoni, J. T. Lopez Navarrete, G. Zerbi, *Solid State Comm.* **1988**, *65*, 625.
[36] M. Gussoni, C. Castiglioni, G. Zerbi, in *Spectroscopy of Advanced Materials* (Eds: R. J. H. Clark, R. H. Hester), Wiley: New York, **1991**, p 251.

